# Calorimetric study of the desorption of the interstitial hydrogen atoms in ferromagnetic $Nd_2Fe_{14}BH_x$ ($x \leqslant 5$) microcrystals

S. Ram* and H. J-Fecht
*Institute of Metal Research, Technical University of Berlin, Hardenbergstrasse-36, D-10623 Berlin, Germany*

S. Haldar and P. Ramachandrarao
*National Metallurgical Laboratory, Jamshedpur 831 007, India*

H. D. Banerjee
*Materials Science Centre, Indian Institute of Technology, Kharagpur-721302, India*
(Received 6 February 1996; revised manuscript received 24 February 1997)

When heating over 300–800 K in a calorimeter, $Nd_2Fe_{14}BH_x$, $x \leqslant 5$, microcrystals desorb the H atoms in six irreversible endothermic signals. They appear at temperatures $T_p \sim 340$, 439 (doubly degenerate), 567, 605, and 653 K at the heating rate $\beta = 15$ K/min, following the modified Kissinger relation $\ln(T_p/\beta) = (E_a/R)T_p^{-1} + \text{const}$, with $R$ the gas constant. The 340 signal has an extremely weak intensity at a slow heating, $\beta \leqslant 40$ K/min, because the H atoms in the involved interstitial site in the sample slowly tunnel to neighboring higher-transition-energy sites. The thermogram at 439 K is the most prominent. It contains two signals which could be resolved by selective isothermal desorptions. These six different identified thermal signals are assigned to the desorptions of the H atoms from six specific $4c$, $16k2$, $16k1$, $4e$, $8j2$, and $8j1$ crystallographic interstitial sites (between the Fe atoms) in the sample, characterized by six different activation energies $E_a$ between 48 and 123 kJ/mol, taking into account their H occupancies $n_i$(H). The distribution of partial enthalpies in the thermal signals (at $\beta = 15$ K/min) determines $n_i(\mathrm{H}) \cong 0$, 6, 5, 2, 5, and 2 H atoms in the respective sites per $Nd_2Fe_{14}BH_x$, $x \sim 5$, crystal unit cell with a total of $4x = 20$ H atoms. It is found that a significant portion of the thermally excited H atoms in these sites, in the process to the desorption, redistributes over neighboring sites of modified energies to keep the H atoms at high temperatures. The redistribution reaction is exothermic. It has been observed separately in $8j2$ and $8j1$ sites at 616 and 684 K (at $\beta = 50$ K/min) in a partially H-desorbed sample in the lower-transition-energy sites by heating it at 583 K. A local redistribution of the interatomic distances and/or the electronic charges occurs within the lattice following the thermal desorption of the H atoms. It results in a monotonically decreasing exothermic (structural relaxation) signal of the rate of the change of the enthalpy, $(\partial H/\partial t)_T$, with time $t$, after the desorption at $t = 0$, following the primary endothermic desorption signal. The results are discussed with simulations of related processes. [S0163-1829(97)07525-5]

## I. INTRODUCTION

The $P4_2/mnm$ tetragonal $R_2Fe_{14}B$ compounds, especially with $R = $ Nd or Pr, constitute the basis of the rare-earth permanent magnets and also provide ideal systems in order to study the complex interplay of the $R$-Fe exchange interaction and the crystal electric field at $R$ sites.[1–6] The anisotropic behavior of these compounds is determined basically by the Fe sublattice which presents a uniaxial anisotropy, although the mechanism of it is not very clear due to the itinerant nature of the $3d$ elements.[7,8] A significant contribution to the anisotropy does result from $R$ with $L \neq 0$ [e.g., $L = 6$ for Nd in the ground electronic state in $Nd^{3+}$ ($4f^3$) oxidation state in $Nd_2Fe_{14}B$[2]]. Nevertheless, the entire $R_2Fe_{14}B$ series has a common feature of the uniaxial anisotropy over $T \geqslant T_{SR}$ up to the Curie temperature $T_C$ [where $T_{SR}$ is called the spin-reorientation transition (SRT) temperature[1–4]], i.e., the magnetic moments in the Fe and $R$ sublattices are collinear, forming a single easy axis of magnetization parallel to the crystallographic $c$ axis. The compounds with $R = $ Nd or Er have a well-defined SRT around 125 and 325 K, respectively,[1,2] in which the easy axis of the magnetization moves away from the $c$ axis with decreasing temperature $T$ below $T_{SR}$.

$R_2Fe_{14}B$ easily intercalates H atoms into the interstitial sites (at 350–450 K in $\sim 1$ bar $H_2$ gas) and forms stable $R_2Fe_{14}BH_x$, $x \leqslant 5$, hydrides. The value of $x \leqslant 5$ varies over the $R$ series in accordance to the atomic radii ($r^{3+}$) and $J$ values of $R$,[9] showing up in a 3.4–5.5 % expansion of the crystal lattice upon the intercalation.[9–11] The hydrogen concentration is not high, but it influences the above interactions by modifying the Fe $3d$ band structure.[12–18] As a result, the H intercalation in $Nd_2Fe_{14}B$ results in a dramatic decrease of the magnetocrystalline anisotropy $H_a$ from 82.5 to 17.6 kOe at 295 K,[18] an increase in the saturation magnetization $M_s$ by 5–11 %,[18–22] an increase in $T_C$ by 5–20 %,[9,20,23] and a shift in the easy axis to easy cone spin-reorientation transition from 125 to 93 K.[9,24]

In spite of the extensive studies of the magnetic and other macroscopic properties of $R_2Fe_{14}BH_x$, $x \leqslant 5$,[9–24] or other similar hydrides,[25–29] very little information is available about the microscopic structure and dynamics of the interstitial H atoms.[24–29] This is mainly due to the lack of the synthesis of a single-phase $R_2Fe_{14}B$ sample by conventional methods of rapid quenching[22,30] or mechanical alloying.[30,31] Such samples often contain an $R$-rich intergranular phase[30–36] with several other minority phases expected according to the $R$-Fe-B equilibrium phase diagram.[30] More-

 

over, it is not easy to intercalate it without causing a severe crystal damage by the reaction with $H_2$ gas in the conventional way of the intercalation.[21,25,27] The lattice expansion and the embrittlement of the sample going along with the hydrogenation fragment it into a refined hydride powder. This often involves a significant dissociation of the sample into the nanocrystalline $\alpha$-Fe, $NdH_{2+\delta}$, $\delta \leqslant 1$, and other dissociation byproducts.[20,21] A few reports using neutron scattering[12] (NS) or other techniques[15,23] sensitive and specific to determine the positions of the interstitial H atoms in the crystal lattice are available on the polycrystalline samples. They are restricted to more or less qualitative studies.[12,15,23]

According to the NS studies,[12] the H atoms in $R_2Fe_{14}B$ occupy the interstitial sites between the Fe atoms, which are distributed in six crystallographically inequivalent sites ($4c$, $4e$, $8j1$, $8j2$, $16k1$, and $16k2$), while the two Nd atoms occupy two sites ($4f$ and $4g$) and the boron occupies only one ($4g$) site.[37,38] In this case, one expects at least six different H sites corresponding to the total of the six different sites for the Fe atoms. However, only four types of H atoms, assigned to the $8j1$ or $8j2$, $16k1$, $16k2$, and $4e$ sites, with the exception of $R=$Ce, in which H does not occupy a $4e$ site, are observed in the NS. The four types of interstitial H atoms have also been identified by thermogravimetric analysis of the partial pressure of the gas in the thermal desorption of H atoms in $Nd_2Fe_{14}BH_x$, $x\sim5$, in a closed volume.[24]

In the present study, we prepared pure $Nd_2Fe_{14}B$ microcrystals by a special technique using a coreduction reaction by Ca in a molten flux.[11] As such, these microcrystals are coated by Ca and other by-products, which help them to intercalate with a controlled amount of nascent hydrogen by washing the coreduced mixture with excess Ca in water in a closed reactor at room temperature (RT). These hydride microcrystals were picked up with the help of a magnetic needle, washed repeatedly by a suitable liquid to wash away the byproduct impurities, and finally dried in a vacuum at RT, as will be described in the experimental section. This yields a pure $Nd_2Fe_{14}BH_x$ sample with a uniform distribution of H atoms in the individual microcrystals with H concentration up to $x\sim5$. With this sample we performed (i) x-ray-diffraction studies probing H desorption at selected temperatures between 300 and 800 K, (ii) magnetic studies using the measurements of $M_s$, $H_c$ (coercivity), and $T_C$, and (iii) thermal studies of selected H desorption by monitoring the partial gas pressure (or volume) or the change in the enthalpy in the desorption as a function of temperature $T$ or time $t$ at an elevated $T$.

Preliminary results of thermograms measured in the thermal desorption of H atoms in $Nd_2Fe_{14}BH_x$, $x\sim5$, microcrystals by differential scanning calorimetry (DSC) are reported in the present article. The results are explored to identify the different interstitial sites of H atoms and to obtain their H occupancies. The kinetics of the desorption of H atoms in the individual sites is modeled and discussed with simulations of related processes.

## II. EXPERIMENTAL PROCEDURE

### A. Synthesis of $Nd_2Fe_{14}BH_x$, $x\sim5$, microcrystals

$Nd_2Fe_{14}BH_x$, $x\sim5$, microcrystals of 10–20 $\mu$m size were prepared by coreduction reaction of $Nd_2O_3$, Fe, and B with calcium metal followed by intercalation with nascent hydrogen, which is produced *in situ* by chemical dissociation of water by washing the product through excess Ca with water at RT. It involves two separate reactions in two successive experiments as follows.

In the first step of the reaction, the powders of $Nd_2O_3$, Fe, and B (all of particle size under 5 $\mu$m and of purity better than 99.9%) were mixed with the necessary amounts (to reduce the $Nd_2O_3$ into Nd metal) of 1–2-mm-sized Ca granules by milling in a steel container together with 2-mm-diameter steel balls under a pure argon atmosphere. An atomic mixing and part of the coreduction reaction. $Nd_2O_3+3Ca \rightarrow 2Nd+3CaO$, occur by deformation during the milling, leading to the formation of a nanocrystalline or amorphous Nd-Fe-B alloy in the mixture. The ferromagnetic $Nd_2Fe_{14}B$ microcrystals grow in the mixture in a subsequent heating at 1300 K. Addition of excess ($\sim$100%) Ca along with $\sim$20 wt. % of a $CaCl_2$-NaCl salt mixture facilitates the growth of the separated $Nd_2Fe_{14}B$ microcrystals in the matrix of the by-products and the additives.

After cooling to RT, the sample was washed with a limited amount of water in a closed reactor filled with a pure argon gas. The Ca in the matrix dissociates the water into nascent hydrogen, $Ca+H_2O\rightarrow Ca(OH)_2+2H$, which very efficiently diffuses in the $Nd_2Fe_{14}B$ microcrystals under the matrix and forms hydride microcrystals at atmospheric pressure. These self-induced exothermic reactions increase the local temperatures, to likely higher than the $bp$ of water, accelerating the hydriding kinetics. Thus special care was taken to obtain $Nd_2Fe_{14}BH_x$, $x\sim5$, microcrystals with a homogeneous H distribution throughout the sample using sufficiently excess Ca in the initial washing and hydriding process. The microcrystals of 10–20 $\mu$m size were recovered with the help of a magnetic needle and sieves of required mesh sizes, carefully washed in fresh water, and then rinsed in ethyl alcohol and $CCl_4$. All these experiments were carried out in an inert (argon) atmosphere to minimize the surface oxidation of the sample. Finally, the sample was dried under vacuum at RT. It was stored under an inert gas before the measurements.

The content of the hydrogen in the sample was determined by thermogravimetric analysis of the desorption of the H atoms. The H atoms commence desorbing off the sample above 325 K, showing up in an increase in the partial gas pressure ($\Delta P$) on heating it in a specific desorption chamber.[11,20] Application of the ideal gas law indicates that a desorption of only 0.5 H atoms per $Nd_2Fe_{14}B$ unit adds an $\sim$0.1 bar gas pressure in the chamber. Thus the analysis of the $\Delta P$ with the corresponding mass of the gas desorbed off the sample (obtained by the difference in the mass of the sample before and after the desorption) confirms that the interstitial gas is pure hydrogen. It precisely determines the amount of H desorbed at selected thermal heatings.

### B. Crystal lattice parameters, microstructure, and magnetic properties

X-ray diffraction, obtained from a position-sensitive detector mounted in Debye-Scherrer geometry with monochromated Cu $K\alpha$ radiation of wavelength $\lambda=0.154\,060$ nm, was used to analyze the formation of the two hydride and

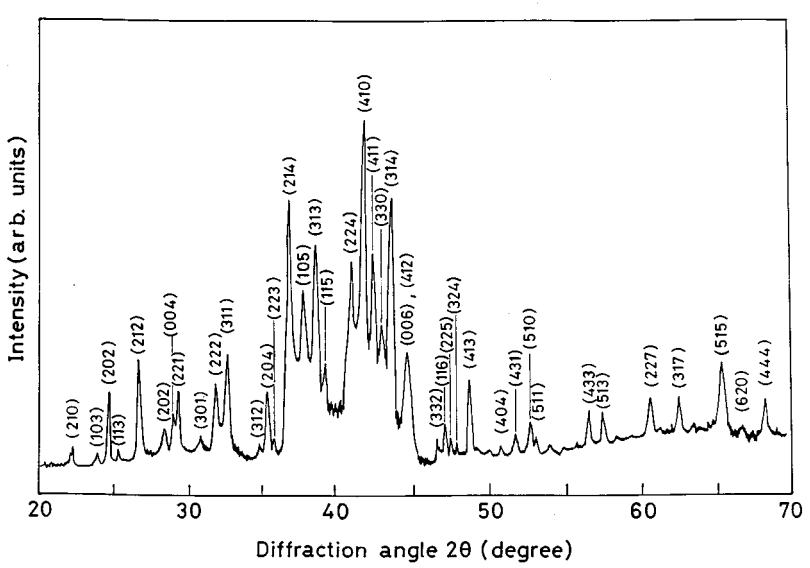


FIG. 1. X-ray-diffraction pattern of a powder sample of $Nd_2Fe_{14}BH_x$, $x\sim5$, microcrystals of 10–20 $\mu$m size.

anhydride samples. All the peaks observed in the x-ray diffractogram (Fig. 1) belong to a single tetragonal crystal structure of the sample. We carefully studied several hydride and anhydride samples, and all have shown the reproducible x-ray diffractograms. None showed impurities of the raw materials or the by-products in a detectable trace. The peaks in the Brag reflections were characteristically sharp in both the hydride and anhydride samples in accordance with the crystal size (10–20 $\mu$m), determined independently by scanning electron micrographs. The positions of these peaks were used to calculate the lattice parameters which are given in Table I. *In situ* studies of the compositional maps with an electron microprobe analyzer confirmed the Fe/Nd ratio to be 7.0 in the $Nd_2Fe_{14}B$ microcrystals throughout the sample. No impurity of Ca or other by-products were found in a detectable amount of 0.1 at.%.

The magnetic properties $M_s$ and $H_c$ were measured with a vibrating sample magnetometer using a magnetic field to 160 kOe. The Curie temperature ($T_C$) was measured by scanning magnetization of the specimen (sealed in a quartz ampoule under vacuum) over 295–800 K at a magnetic field of 1–2 kOe on a Faraday balance.[20,22] Our data of $T_C$ fairly agree with the standard values (cf. Table I). However, the $M_s$ values are $\sim$3% lower, presumably due to a thin grain-surface passivation (which is nonmagnetic or weak ferromagnetic compared to the primary phase[11]) formed during the washing process.

### C. DSC measurements

A Perkin-Elmer DSC-7 calorimeter was used to study the thermograms in desorption of the H atoms in the $Nd_2Fe_{14}BH_x$, $x\sim5$, microcrystals. A 20–50 mg sample, sealed in an aluminum pan (which is nonpermeable for hydrogen) with an aluminum lid of similar diameter using a standard press, was scanned under a constant flow of argon in the calorimeter against a reference pan sealed with the lid. The data were collected by simultaneously deducing a predetermined base line from the scan programmed through a computer. Scanning rates ($\beta$) usually ranged from 10 to 40 K/min, though some slower and faster scans were performed as part of a Kissinger analysis. The isothermal measurements were obtained at selected temperatures between 400 and 750 K. In this case, the specimen was heated from RT to the predetermined temperature by a given heating rate and held in order to measure the heat flow $(\partial H/\partial t)_T$ in the H desorption as a function of time $t$.

## III. RESULTS AND DISCUSSION

### A. Magnetic properties

A pure sample of $Nd_2Fe_{14}BH_x$, $x\sim5$, microcrystals of 10–20 $\mu$m size has saturation magnetization $M_s = 179$ emu/g, which is $\sim$9.8% larger than the value for the anhydride at RT. This value compares well with the $M_s = 168$ emu/g value for $Nd_2Fe_{14}B$ single crystals[1,3,4] or a $M_s = 185$ emu/g value reported for a $Nd_2Fe_{14}BH_x$, $x\sim5$, hydride sample obtained by heating the anhydride with $H_2$ gas.[18,20,22] It is evident from these results that our sample of $Nd_2Fe_{14}BH_x$, $x\sim5$, microcrystals do not have a significant amount of by-product impurities. As mentioned in the experimental section, all of the diffraction peaks in the typical x-ray diffractogram, shown in Fig. 1, are indexed assuming a single $P4_2/mnm$ tetragonal $Nd_2Fe_{14}BH_x$, $x\sim5$, phase with the lattice parameters $a = 0.893$ nm and $c = 1.232$ nm. The possible oxide impurities, if any, very sensitively lower the total $M_s$ value of the sample. For example, a thin [$\sim$0.05 $\mu$m (Ref. 20)] oxide (or hydroxide) grain-surface passivation (GSP) in a sample of as small as $\sim$1 $\mu$m microcrystals (with larger surface area) has reduced the $M_s$ value at $\sim$145 emu/g (Refs. 11 and 20) when compared to 179 emu/g for the present sample of significantly larger 10–20 $\mu$m microcrystals. Also, in the 1 $\mu$m microcrystals, the GSP adds a total oxygen content of $\sim$2 at.% only as analyzed using the electron microprobe analysis. A presumably smaller $\leqslant$0.1 at.% oxygen impurity (see the experimental section) in the 10–20 $\mu$m microcrystals accords to their larger $M_s\sim179$ emu/g value.

The 10–20-$\mu$m-sized $Nd_2Fe_{14}BH_x$, $x\sim5$, microcrystals are far larger than the effective ferromagnetic single-domain size $\sim$0.2 $\mu$m.[11] These are therefore multidomain ferromag-

TABLE I. Crystal lattice parameters and magnetic properties of $Nd_2Fe_{14}BH_x$, $x \leqslant 5$, microcrystals and related alloys.

| Sample | Lattice parameters | | Magnetic properties | | | |
|---|---|---|---|---|---|---|
| | $a$ (nm) | $c$ (nm) | $M_s$ (emu/g) | $H_c$ (kOe) | $T_C$ (K) | $H_a$ (kOe) |
| (1) Crystalline $Nd_2Fe_{14}BH_x$[a] ribbons | | | | | | |
| (a) $x=0$ | 0.880 | 1.220 | 168 | | 588 | 82.5 |
| (b) $x\sim5$ | 0.893 | 1.234 | 185 | | 645 | 17.6 |
| (2) $Nd_2Fe_{14}B$ single crystals[b] | | | 168 | | 586 | $\sim$95 |
| (3) $Nd_2Fe_{14}BH_x$ microcrystals | | | | | | |
| (a) $x=0$ | 0.880 | 1.218 | 163 | $\leqslant$0.500 | 593 | 85.0[c] |
| (b) $x\sim5$ | 0.893 | 1.232 | 179 | $\leqslant$0.050 | 645 | 16.5[c] |

[a]References 18, 20, and 22.

[b]References 1, 3, and 4.

[c]The data are taken from our unpublished work not included here.

netic particles. As a result, they exhibit a low coercivity $H_c \sim 50$ Oe ($\sim$500 Oe for the anhydride) at RT. The low $H_c$ value is consistent with the low value for the magnetocrystalline anisotropy $H_a = 16.5$ kOe in comparison to 85.0 kOe for the anhydride. As mentioned above, the H atoms modify the magnetic parameters of the anhydride by modifying primarily the Fe-Fe and Fe-$R$ exchange interactions.[9–24] The modified (enhanced) exchange interactions in the hydride have a direct correlation with the Curie temperature[9,20,23] which is found to be enhanced to $T_C = 645$ K in comparison to $T_C = 593$ K for the anhydride. Other details about the magnetic properties for the typical hydride and anhydride samples are summarized in Table I.

### B. Thermograms in the thermal desorption of H atoms

Six irreversible endothermic signals, overlapping one another, appear between 325 and 800 K (Figs. 2 and 3) in the desorption of H atoms in $Nd_2Fe_{14}BH_x$, $x\sim5$, microcrystals during heating from RT in the calorimeter. The average positions as well as the intensities of these signals purely depend on the rate of the heating $\beta$ and other experimental conditions. As a result, apparently, only four thermograms are distinguished at 439, 567, 605, and 653 K at a slow heating rate of $\beta = 15$ K/min. The peaks shift to higher temperatures with increasing $\beta$, as high as 100 K/min used in the present example, as can be seen from comparison of the thermograms recorded at representative $\beta$ values in Fig. 3. Another endothermic signal (marked by $a$ in Fig. 3) shows up with a significant intensity at $\sim$350 K in the fast scanning at $\beta \geqslant 40$ K/min. It is mixed with the following intense and broad endotherm impossible to resolve its features by scanning it at different $\beta$. The broad endotherm contains two different signals (marked by $b$ and $c$ in Fig. 3) which could be distinguished with the help of the isothermal measure-

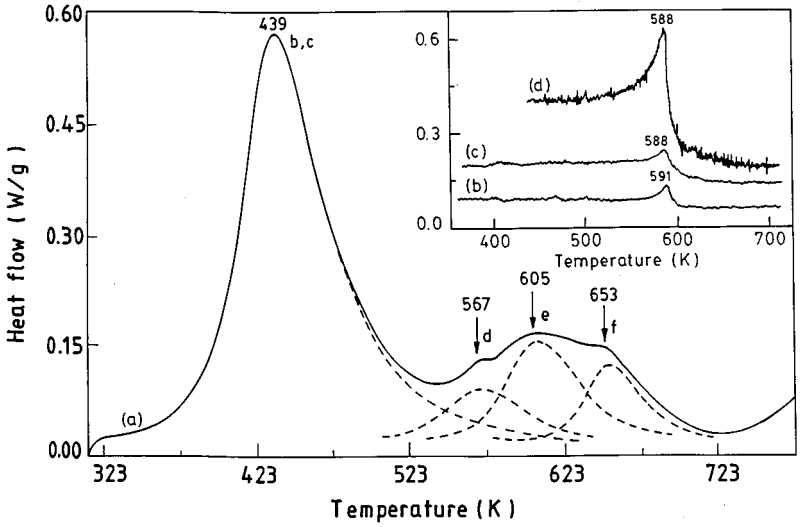


FIG. 2. (a) Thermogram in the desorption of H atoms in $Nd_2Fe_{14}BH_x$, $x\sim5$, microcrystals at 15 K/min heating rate. The dashed curves are the guidelines for the endothermic signals $b$ (or $c$), $d$, $e$, and $f$ overlapping one another. In the inset are compared the thermograms from (b) the anhydride or (c) a dehydrided hydride (a) sample. The thermogram (d) is obtained by reheating the sample after the scan (c) at an $\sim$5 times magnified scale of the $Y$ axis in the other thermograms.

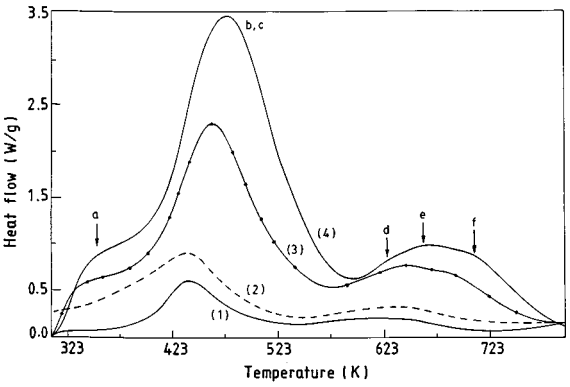


FIG. 3. Thermograms showing the $\beta$ dependence of H desorption in $Nd_2Fe_{14}BH_x$, $x\sim5$, measured at selected scanning rates ($\beta$): (1) 15 K/min, (2) 25 K/min, (3) 60 K/min, and (4) 100 K/min.

ments as discussed below. It adds the total numbers of the identified signals to altogether six. These are labeled as $a$, $b$, $c$, $d$, $e$, and $f$ in increasing order of their positions in temperature (or energy $kT$, with $k$ Boltzmann's constant) in the thermogram, representing the desorption of the H atoms from six specific interstitial sites in the sample.

In a separate experiment, a thermogravimetric analysis of the mass and the partial pressure (or volume) of the gas desorbing off the sample, on heating it in a closed chamber,[11,20] confirms it to be the pure hydrogen. Also nitrogen forms the interstitial $Nd_2Fe_{14}BN_\delta$, $\delta\leqslant2.5$, nitrides,[39] but these are easily identified by thermogravimetric analysis. Oxygen is another possible impurity in this example. It exists presumably as an oxide or hydroxide of the Nd or Fe constituent elements of the sample as part of the grain-surface passivation (GSP). The hydroxide, if any, decomposes to the oxide, e.g., $2Nd(OH)_3\rightarrow Nd_2O_3+3H_2O$, at high temperatures above 700 K.[20] It does not obscure the features of the strong H-desorption thermograms in this example, in which the total content of O atoms is negligibly small, $\leqslant0.1$ at.%.

An anhydride $Nd_2Fe_{14}B$ sample, prepared under identical conditions, does not exhibit a significant thermal signal in this region, except a very weak endothermic peak at 591 K [Fig. 2(b)]. The enthalpy $\Delta H=0.63$ J/g in this peak is $\sim3$ orders of magnitude smaller than the total $\Delta H$ in the six H-desorption signals. This peak refers to the Curie transition ($T_C$) of $Nd_2Fe_{14}B$.[18,20] Also, a dehydrided hydride sample by heating to high temperatures 850 K exhibits a similar $T_C$ signal in thermogram $c$ or $d$ in Fig. 2 at a similar temperature. It is evident from these results that the GSP or other by-product impurities, if any, are not enough to contribute additional heat flow signals in this region that could be analyzed by the present methods. Obviously, qualitatively, no hydrogen comes from other H-bonding sites due to the GSP or the by-product impurities, if any. Moreover, it is difficult to comment with the present data whether or not the GSP causes structural changes of the grain surfaces that may affect the desorption of the H atoms in the primary H-bonding sites.

The large bandwidths $\Delta T_{1/2}$, e.g., $\Delta T_{1/2}\sim65$ K in the thermogram $b$ or $c$ at 439 K in Fig. 2, in the primary H-desorption signals indicate thermal excitations of the H atoms through a large number of localized H energy levels in each of the six interstitial H sites in $Nd_2Fe_{14}BH_x$, $x\leqslant5$. This wide spectrum of the energy levels is not easy to scan by heating the sample at a single temperature to excite the successive desorptions of H atoms from the successive H energy levels over a time scale in an isothermal scanning. Some of the H atoms in the low-energy interstitial sites excite at temperatures as low as 325 K, but most H energy levels excite only at higher temperatures to show up a desorption thermogram to be measured by the calorimeter. In this case, in order to analyze the individual H-desorption signals by the isotherms, we scanned series of isotherms in successive excitations of controlled numbers of the H energy levels at selected temperatures. Thus a single sharp symmetric isotherm [Fig. 4(a)] in presumed signal $b$ appears during heating a sample over 303–418 K by $\beta=150$ K/min and held. At this low temperature, no higher-energy H-desorption signals appear. After 90 min isothermal heating at 418 K, the sample was rapidly (150 K/min) cooled to 303 K. Then the isotherm, reproduced in Fig. 4(b), was obtained under the same conditions as in Fig. 4(a). It still has the shape of a single sharp symmetric signal, but the enthalpy $\Delta H\sim61$ J/g is reduced by a factor of $\sim2$ as a result of the H desorption which occurred during the first heating cycle.

In this case, in order to demonstrate the two presumed components of this thermogram, we recorded a thermal activation spectrum of the desorption of H atoms by heating the sample in successive steps at 398, 428, 448, 478, 533, and 583 K using a common heating rate of 100 K/min over the intermediate temperatures and 1.2, 1.2, 1.2, 1.5, 1.5, and 90 min holds at respective temperatures. The relative integrated intensities of the six isotherms in this thermal activation spectrum vary in a systematic 100:81:58:60:75:61 order in accordance with the desorption of H atoms from two different interstitial sites. Thus the first three isotherms [Fig. 5(a)] represent part of the intensity distribution of H desorption in the presumed signal $b$, while the other three isotherms are in part of signal $c$. The two signals of $\Delta H$ (total 29 J/g) in a 5:4 ratio are clearly indicated in the thermogram in Fig. 5(b) after smoothening the data points (to a level so that they no longer show the peaks at the intermediate excitation temperatures) by a standard program available with the calorimeter. This represents a statistical distribution of the data points in a continuous thermal activation spectrum of the desorption of the H atoms over 303–583 K. Thus we studied several sets of isotherms with different combinations of intermediate temperatures and all demonstrated a reduced thermogram with the doublet structure intrinsic to the two overlapping signals $b$ and $c$. The subsequent isothermal signal $d$, with $\Delta H\sim46$ J/g, occurs later at temperatures as low as 583 K [Fig. 5(c)]. The isotherms in the other two presumed signals $e$ and $f$ occur (with $\Delta H=115$ and 60 J/g, respectively) on heating to further higher temperatures of 610 K. These $b$, $c$, $d$, $e$, and $f$ isothermal signals, although they show higher $\Delta H$ by as much as a factor of 2.1, have basically the same 100:80:28:71:37 ratio of $\Delta H$ values as (100:80:30:73:37) in the isochronal ($\beta=15$ K/min) measurements.

The values of $\Delta H$ in the $a$, $b$, $c$, $d$, $e$, and $f$ signals in either method of isochronal or isothermal heating represent the numbers of H atoms desorbed from the associated interstitial H sites in $Nd_2Fe_{14}BH_x$, $x\leqslant5$, if the effects of the

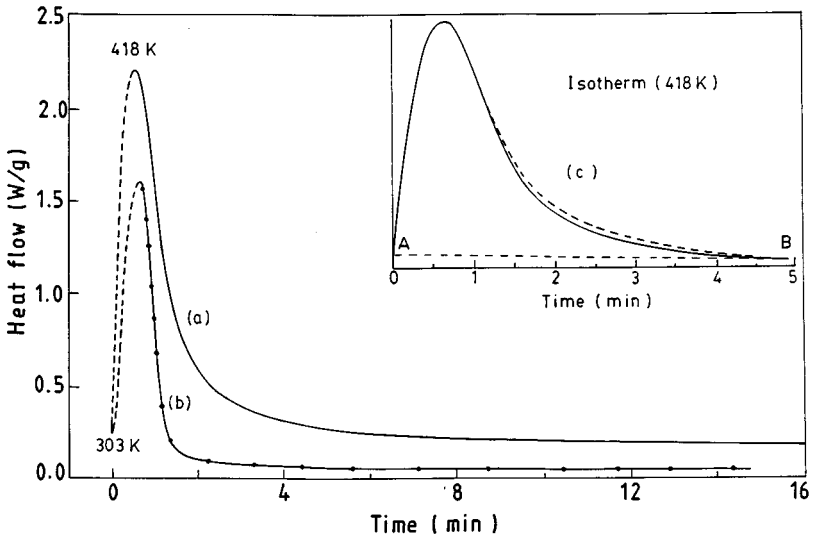


FIG. 4. (a) Thermogram in a controlled H desorption in $Nd_2Fe_{14}BH_x$, $x\sim5$, in heating from 303 to 418 K at $\beta=150$ K/min and held for 90 min at 418 K. The sample was cooled (150 K/min) to 303 K and then thermogram (b) was obtained by reheating it at 418 K under the same conditions as in (a). The dashed curves represent the parts of the thermograms measured during the isochronal heating over 303–418 K. Thermogram (c), which is an expansion of thermogram (a), is well reproduced (dotted curve) using the simulation with $\alpha=1$, $n=1.6$, and $b=0.72$ min$^{-1.6}$, with the observed $\Sigma\Delta H_i=133.5$ J/g value, in Eq. (12).

reordering of H atoms are neglected. In this approximation, they may be utilized as independent experimental variables to determine the occupation numbers of H atoms in the respective sites by the relation

$$n_i(H)=\frac{4xf_i(\Delta H_i)}{\Sigma_{i=1}^{6}f_i(\Delta H_i)} \tag{1}$$

per crystal unit cell (with $4x$ H atoms). In this relation, $f_i$ is the fractional number of H atoms desorbed with the change in the enthalpy $\Delta H_i$ in signal $i$ and $\Sigma\Delta H_i$ is the total enthalpy in the resultant thermogram of all the six signals. Assuming the optimum value of $f_i=1$ or any other common value of it in all six signals, Eq. (1) simplifies to

$$n_i(H)=\frac{4x\Delta H_i}{\Sigma_{i=1}^{6}\Delta H_i}. \tag{2}$$

It determines the value of $n_i(H)$ in terms of a single variable $\Delta H_i$. The values of $\Delta H_i$ used to calculate the $n_i(H)$ in Eq. (2) were analyzed by fitting the observed isochronal thermogram with six individual signals. The total $\Delta H=140$ J/g (at $\beta=15$ K/min) in the broad thermogram of two signals $b$ and

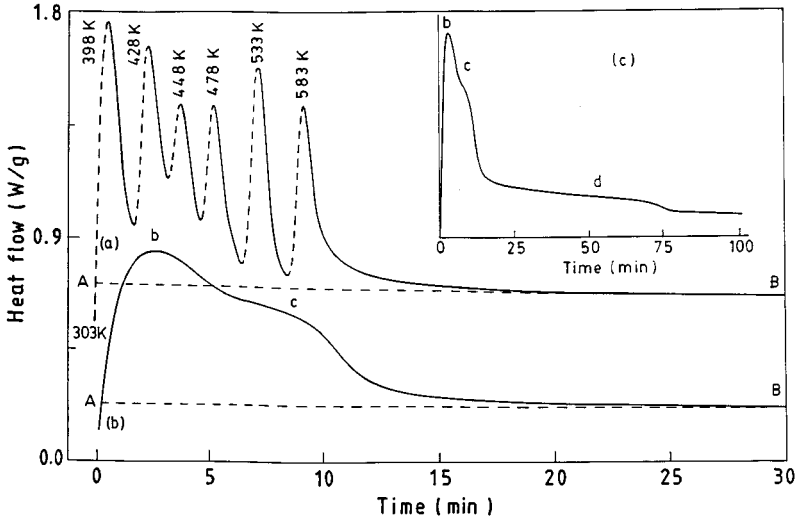


FIG. 5. (a) A thermal activation spectrum of the desorption of H atoms in $Nd_2Fe_{14}BH_x$, $x\sim5$, measured in successively heating a sample at 398, 428, 448, 478, 533, and 583 K for 1.2, 1.2, 1.2, 1.5, 1.5, and 90 min, respectively, using a common $\beta=100$ K/min heating rate throughout the range. The dashed curves represent the parts of the thermograms measured during the isochronal heating over the involved temperatures. Thermogram (b) is shown after smoothening the data points to represent a realistic picture of it in a continuous thermal activation over the 303–583 K range. A complete thermogram (b) is reproduced in (c).

TABLE II. DSC signals and the kinetic parameters derived from the DSC signals in the desorption of interstitial H atoms and the effects of H atoms on the magnetic hyperfine fields $B_{HF}$ at Fe sites in $P4_2/mnm$ tetragonal $Nd_2Fe_{14}BH_x$, $x\sim5$, crystals with $z=4$ formula units (68 atoms excluding H atoms) per crystal unit cell.

| DSC signals | Peak temperature[a] $T_p$ (K) | Enthalpy $\Delta H$ (J/g)[a] | Occupancy of H atoms $n_i$(H)[b] | Activation energy $E_a$ (kJ/mol) | Occupancy of Fe atoms $n_i$(Fe)[c] | Crystallographic sites of H/Fe atoms[c,d] | Hyperfine field $B_{HF}$ (kOe)[d] |
|---|---|---|---|---|---|---|---|
| *a* | not clear[e] | ~0 | ~.0(0) | ---- | 4 | 4*c* | 272(273) |
| *b* | 439 | 78 | 6.3(6) | 49 | 16 | 16*k*2 | 328(304) |
| *c* | 439 | 62 | 5.0(5) | 49 | 16 | 16*k*1 | 300(285) |
| *d* | 567 | 23 | 1.8(2) | 48 | 4 | 4*e* | 329(312) |
| *e* | 605 | 57 | 4.6(5) | 123 | 8 | 8*j*2 | 358(343) |
| *f* | 653 | 29 | 2.3(2) | 113 | 8 | 8*j*1 | 271(270) |
| Total | | 249 | 20(20) | | 56 | | |

[a]The peak temperature $T_p$ and $\Delta H$ values are reported for the thermogram measured at 15 K/min heating rate.
[b]Crystallographically feasible approximate integral values of $n_i$(H) are given in the parentheses.
[c]After Herbst *et al.* in Ref. 37.
[d]After Cadogan and Coey in Ref. 23. The values of $B_{HF}$ for the anhydride are given in the parentheses.
[e]This particular signal does not appear in the slow heating rate of 15 K/min.

*c* at 439 K (Fig. 2) is divided in a 5:4 ratio, as determined by the isothermal measurements. Thus the total $\Delta H$ is distributed in a 0:100:80:30:73:37 ratio over the six signals. From neutron-diffraction studies of $Y_2Fe_{14}BD$, at RT, Dalmas de Reotier *et al.*[12] reported that H atoms first fill the 4*e* sites. Then the 8*j*1 or 8*j*2, 16*k*1, and 16*k*2 sites are simultaneously and progressively filled up to $x=2.5$ D atoms, resulting in site occupancies in the 26:100:80:54 ratio. This supports the present results, by excluding the thermal signals *a* and *f*, with the final $\Delta H$ distribution in the 30(d):100(b):80(c):73(e) order. The high-temperature *e* and *f* signals in the present case have relatively large intensities due to a significant refilling of these sites by an internal reordering of H atoms at these temperatures. Small H occupancies at RT in the sites (4*c* and 8*j*1) related to the thermal signals *a* and *f* induce small ~1 kOe (15–24 kOe in the other sites) changes in the magnetic hyperfine fields (cf. Table II) of the anhydride at RT.[23]

The dependence of the peak temperature $T_p$ in these thermal signals on the scanning rate $\beta$ proves that the desorption of H atoms in this example is a kinetic process. It can be utilized to analyze the kinetics of the desorption of H atoms in the identified interstitial sites in $Nd_2Fe_{14}BH_x$, $x\leqslant5$, using a first-order single activated thermal process in each case, as assumed in the original Kissinger relation[40]

$$\ln\left[\frac{T_p^2}{\beta}\right]=\left[\frac{E_a}{R}\right]T_p^{-1}+\text{const}, \tag{3}$$

where $E_a$ is the activation energy and $R$ is the gas constant. This relation applies accurately only when the H desorption is dominated by a single nondegenerate thermally activated process with an Arrhenius temperature dependence. For a higher-order desorption process, which has no nucleation barrier, $T_p$ will be in principle independent of $\beta$. Application of this relation to such an example will result in an ambiguously high estimate of $E_a$.

As discussed earlier,[24] the variation of $T_p$ with $\beta$ in the thermal desorption of H atoms in $R_2Fe_{14}BH_x$, $x\leqslant5$, and similar hydrides is usually a more satisfactorily described with a modified Kissinger relation[41]

$$\ln\left[\frac{T_p}{\beta}\right]=\left[\frac{E_a}{R}\right]T_p^{-1}+\text{const} \tag{4}$$

than with the original relation (3). Note that the modified and the original Kissinger relations both are the purely empirical relations derived from an Arrhenius temperature dependence. Both are used traditionally as a vehicle to determine the value of the activation energy $E_a$ of a kinetic process using the experimental variables $T_p$ and $\beta$. As a matter of fact, our $\ln(T_p/\beta)$ vs $T_p^{-1}$ plots, shown in Fig. 6, thus present the best fit to the experimental data points using the straight line. The slope $(E_a/R)$ of the straight line provides an average value of $E_a$, which was found to be 49, 48, 123, or 113 kJ/mol for

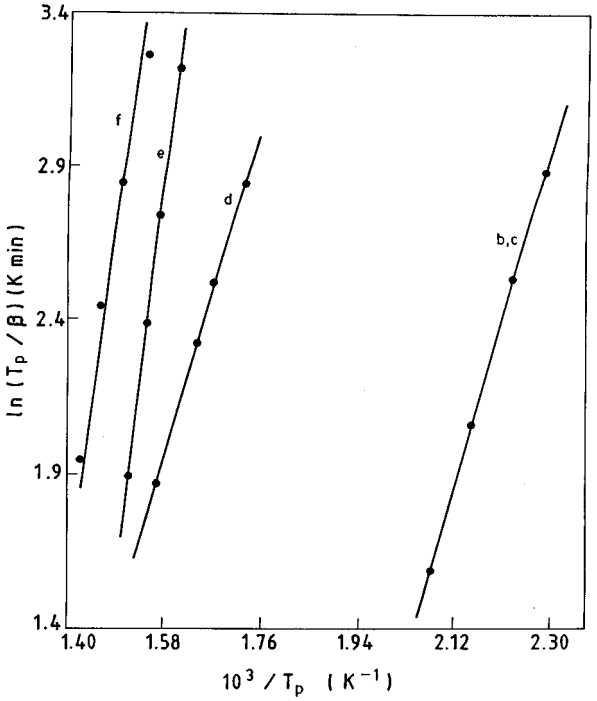


FIG. 6. $\ln(T_p/\beta)$ vs $T_p^{-1}$ plots for the endothermic H-desorption signals *b* (or *c*), *d*, *e*, and *f* in $Nd_2Fe_{14}BH_x$, $x\sim5$.

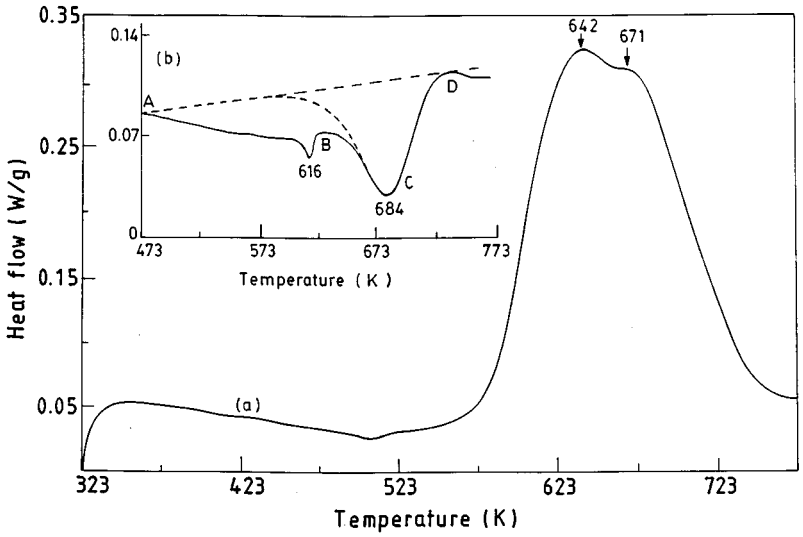


FIG. 7. A doublet thermogram (a) in the signals *e* and *f* measured during heating a preheated $Nd_2Fe_{14}BH_x$, $x\sim5$, sample [at 523 K for 10 min by a fast (100 K/min) heating over the lower temperatures and then rapidly cooled to 303 K] at $\beta=40$ K/min. Thermogram (b) is scanned with a new sample at $\beta=50$ K/min after a preheating at a slightly higher 583 K temperature for 90 min.

the four resolved thermal signals *b* (or *c*), *d*, *e*, and *f*, respectively, in the $Nd_2Fe_{14}BH_x$, $x\sim5$, sample.

### C. Selected desorption and reordering of H atoms

A significant portion of H atoms excited in the localized H energy levels in $Nd_2Fe_{14}BH_x$, $x\leqslant5$, undergoes redistribution over the mobile interstitial sites if heated above RT. The desorption of H atoms from the $4c$ site in the thermal signal *a*, which shows up with an enhanced intensity around 340 K at a fast heating, $\beta\geqslant40$ k/min, presents a good example of the H redistribution with the neighboring sites. At slow heating, the H atoms in this site slowly tunnel to the neighboring higher transition-energy ($kT$) sites and therefore impart a reduced H-desorption intensity in this signal (*a*). The H-desorption-induced H vacancies at high temperatures offer another type of reordering of the H atoms at elevated temperatures. To demonstrate this type of reordering of H atoms in the H-desorption-induced H vacancies, we annealed a $Nd_2Fe_{14}BH_x$, $x\sim5$, sample at 523 K for 10 min, to desorb the H atoms in the lower-transition-energy signals before the signal *d*, by heating from 303 to 523 K at $\beta=150$ K/min and cooled (150 K/min) it back to 303 K, and then reheated it to scan the final thermogram, shown in Fig. 7(a) over 303–800 K at $\beta=40$ K/min. The annealing at 523 K did not induce the signal *d* (which appears at temperatures as low as 583 K [Fig. 5(c)]), but it apparently does not occur in the isochronal thermogram in Fig. 7(a), which shows only two modified signals *e* and *f* at 642 and 671 K with a decreased value of $\Delta H$ from 85 to 44.9 J/g. The results prove that H atoms in the interstitial site ($4e$) in signal *d* readily redistribute over the lower-energy H vacancies (in the signals *a*, *b*, or *c*) while cooling the sample after part of H desorption at 523 K and therefore they do not show up anymore in the same thermal signal in the reheating cycle.

Another thermogram, recorded after annealing a $Nd_2Fe_{14}BH_x$, $x\sim5$, sample at slightly higher temperature 583 K for 90 min in a similar fashion exhibits an exothermic signal [labeled *ABCD* in Fig. 7(b)], with $\Delta H=-9.5$ J/g, having two peaks at 616 and 684 K (which compare well with the positions for the endothermic signals *e* and *f*) superimposed over a background. These new signals are indicative of the reordering of H atoms in the high-energy H vacancies in signals *e* and *f* during the heating. In a ternary $ErFe_2D_{3,2}$ deuteride, Krill *et al.*[27] also observed two exothermic signals which had followed two endothermic signals in the desorption of the D atoms over 330–700 K. The positions of the peaks in the desorption as well as the redistribution of H atoms in $Nd_2Fe_{14}B$ primarily depends on the experimental conditions of the concentrations of H atoms in the involved interstitial sites and the total H content in the sample. The H desorption in signals *e* and *f*, which appear at 642 and 671 K for $x\sim5$, thus had shifted to ~700 K at $x\sim2$.

Thermogravimetric analysis of the desorption of H atoms in $Nd_2Fe_{14}BH_x$, $x\leqslant5$, determines that 10–20 % of H is still present in the sample at temperature as high as 700 K. The sample after H desorption at 700 K for 30 min in the calorimeter thus still measures a larger crystal lattice volume $V=0.957$ nm$^3$ as compared to 0.943 nm$^3$ in the anhydride. The last H atoms in the sample maintain a high $M_s=171$ emu/g value compared to 163 emu/g in the anhydride (179 emu/g in the hydride with $x\sim5$) as measured at 295 K. On further heating, these H atoms partly desorb and partly redistribute into thermally mobile high-energy H vacancies according to the experimental conditions. For example, when heating to 723 K, they exhibit a two-step H desorption as a function of time (cf. thermograms *a* and *b* in Fig. 8), showing two endothermic signals at 8 s ($\Delta H=6.5$ J/g) and 168 s ($\Delta H=10.0$ J/g) after $t=0$ at the moment the sample reached at 723 K. The first signal is rather sharp with a half-bandwidth (the full width at the half peak intensity) $\Delta t_{1/2}=15$ s, while the other is broad, $\Delta t_{1/2}\sim250$ s. The rate of H desorption in this case is progressively enhanced in successively heating a fresh sample to (c) 623 K ($\Delta H=0.28$ J/g), (d) 673 K ($\Delta H=4.4$ J/g), and (e) 723 K ($\Delta H=6.5$ J/g) in Fig. 8.

The H reordering as well as the H desorption both involve an instantaneous thermal excitation of H atoms through high-energy thermal states in the involved interstitial sites. It results in an instantaneous change in the equilibrium positions of the atoms in the lattice at the moment the H atoms redis-

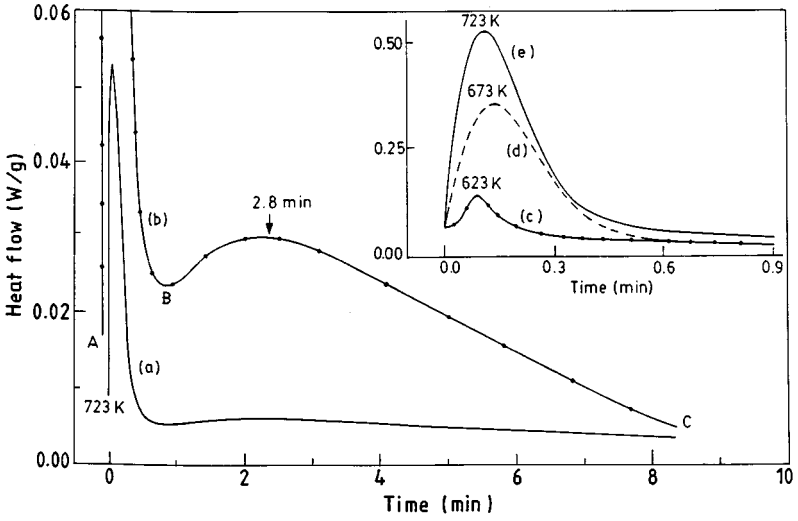


FIG. 8. A two-step isothermal desorption of the last H atoms at 723 K in $Nd_2Fe_{14}BH_x$, $x\sim5$, using a slow (10 K/min) heating over the lower temperatures. Curves *a* and *b* are the same shown at the two different scales of the *Y* axis. The indicated scale, which applies for curve *b*, is an $\sim10$ times expansion of that in curve *a*. Isotherms (c), (d), and (e) represent the desorption of H atoms during the initial isothermal heatings in successive steps at 623 K (40 min), 673 K (12 min), and 723 K (10 min) in a similar fashion, using a common 100 K/min heating rate between 623 and 723 K and the slow (10 K/min) heating over the lower temperatures.

tribute over the mobile H vacancies, or jump off the lattice, by causing an instantaneous change in the momentum of the system. The final atoms in the lattice subsequently relax towards their equilibrium positions (or energy $E_0$ at a given temperature) in the lattice by releasing the excess thermal-structural energy. As shown in Fig. 9, this results in a monotonically decreasing exothermic structural relaxation signal[42,43] of the rate of change of the enthalpy, $(\partial H/\partial t)_r$, as a function of time $t$ at elevated temperature. It is intimately mixed up with the primary thermal signals (in the H-redistribution reaction) in Fig. 7(b) by obscuring their final structures. The heat flow at point $D$ in the exotherm $ABCD$ in Fig. 7(b) thus stand higher than the value at the starting point $A$. The selected inclusions of H atoms into the energetically favorable sites and the resulting reordering of the microstructure are likely universal in any solid sample having mobile interstitial atoms.

### D. Modeling of the thermal signals in the desorption of H atoms

The numbers of the occupied energy levels $N(T,t)$ of H atoms in the interstitial sites in $Nd_2Fe_{14}BH_x$, $x\sim5$, at temperature $T>T_0$ (where $T_0$ is the critical temperature below which the H atoms are strictly immobile in the interstitial sites) can be written in a simple form using the usual exponential relations as follows:

$$N(T,t)=\sum_{i=0}^{\infty} N_i(T_0)\exp(\Delta E_i/kT) + \alpha\sum_{i=0}^{\infty}\Delta N_i\{1-\exp(-bt^n)\} + (1-\alpha)\sum_{i=0}^{\infty}\Delta N_i\exp\{-(t/\tau)^{\eta}\}. \quad (5)$$

The first term in this relation describes the Boltzmann-type thermal distribution and the thermal excitation of H atoms in energy levels $N_i$ (with energy $E_i$) through the difference $\Delta E_i$ between the H energy levels on neighboring interstitial sites, while the second and third terms represent the transformation of H atoms excited in mobile energy levels, $\Delta N = N(T)-N(T_0)$, by the H redistribution (or desorption) reactions into thermally induced H vacancies at $T>T_0$, followed by the structural relaxation (SR) of the crystal lattice. The SR of the crystal lattice occurs subsequent to H desorption through the excited H energy levels $E_i$, approaching the equilibrium configuration of the atoms in the lattice in the equilibrium energy state $E_0$ at elevated temperatures. Relaxation in a physical quantity along with time after a sudden change in the equilibrium condition is likely universal in any solid system. Other terms in Eq. (5) refer to $b$ or $n$ as the rate constant or the order of the H redistribution (or desorption) reaction, $\tau$ the relaxation time, and $\eta$ an exponent. $\alpha$ and $1-\alpha$ are the fractional ratios of $\Delta N$ shared between the two processes. Unfortunately, the values of most of these parameters are not known independently and the activation energy in the H redistribution reaction in correlated energy levels within the nearest-neighboring interstitial sites is expected to be small enough to rule out classical hopping and it rather introduces a sort of chemical tunneling process. A comparison of the results with the phonon-assisted tunneling of small polarons, which successfully describes the motion of muons or H protons in metals, implies a hopping rate[44]

$$\tau^{-1}(T)=\nu_0\exp(-\Delta E/kT), \quad (6)$$

with

$$\nu_0=A_iT^{-1/2}, \quad (7)$$

and

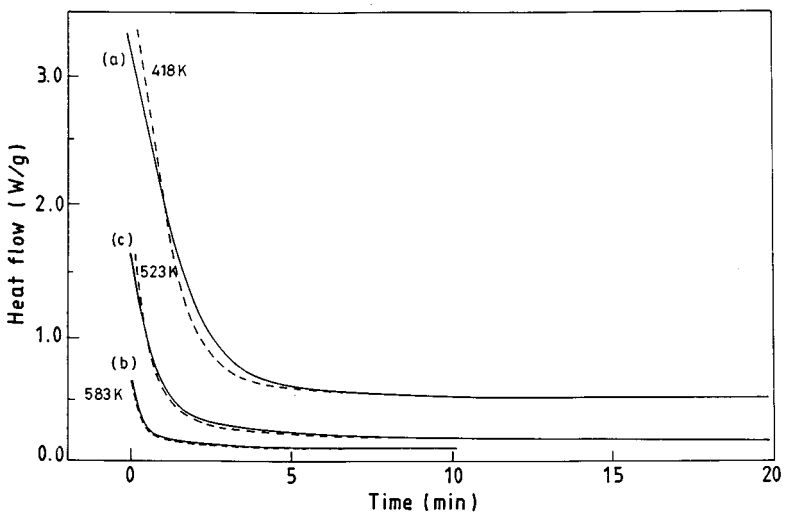


FIG. 9. Simulations (dashed curves) of the extended isotherms at 418, 523, and 583 K of Figs. 4(a), 5(b), and 7(a) obtained by the formalism of the structural relaxation in Eq. (11) using $\alpha=1$ and $\eta=0.6$ with the other parameters of (a) $\tau=25$ s and $\Sigma\Delta H_i=480$ J/g, (b) $\tau=21$ s and $\Sigma\Delta H_i=16$ J/g, and (c) $\tau=25$ s and $\Sigma\Delta H_i=144$ J/g, respectively.

$$A_i=J^2(4\hbar^2\Delta Ek/\pi)^{-1/2}, \tag{8}$$

where $J$ is the tunneling matrix and $\Delta E$ is the difference between the H energy levels on the neighboring interstitial sites.

Thermodynamically, the transformation of $\Delta N$ in Eq. (5) occurs by the redistribution of the internal energy $E$ or by the desorption of the partial volume $V$ (or a combination of both) of the sample following the first law of thermodynamics:

$$H=E+PV, \tag{9}$$

where the pressure $P$ and enthalpy $H$ have their usual meanings. The redistribution of H atoms within the interstitial sites in $Nd_2Fe_{14}BH_x$, $x\leqslant 5$, occurs primarily by a redistribution in $E$, while the desorption of H atoms occurs by leading to a change in $V$ as well as $E$. The H vacancies in the desorbed H atoms modify $E$ by modifying the configuration of the final atoms in the lattice. In the case of pure H desorption, Eq. (9), which, in principle, deals with the total enthalpy in a closed system, simply represents a partial desorption of the enthalpy through the desorption of the mass (or the partial volume $V$) of the sample so that the total enthalpy is conserved. In this case, we can assume, to a first approximation, that the rate of the transformation $(\partial N/\partial t)_T$ of $\Delta N$ with $t$ at a given $T$ is proportional to $(\partial E/\partial t)$ and/or $(\partial V/\partial t)$. Thus the substitution of $(\partial E/\partial t)=m(\partial N/\partial t)$ and $(\partial V/\partial t)=n(\partial N/\partial t)$ in the partial differentiation of Eq. (9) yields

$$\left[\frac{\partial N}{\partial t}\right]_T=\frac{1}{m+nP}\left[\frac{\partial H}{\partial t}\right]_T, \tag{10}$$

with $m$ and $n$ the constants of the proportionalities.

A substitution of the value of the $(\partial N/\partial t)_T$ from Eq. (10) in the partial differentiation of Eq. (5) with respect to $t$ implies an expression

$$\begin{aligned}(\partial H/\partial t)_T=&\sum_{i=0}^{\infty}\Delta H_i(T_0)[\exp\{\Delta E_i/kT\}]\{\partial\Delta E_i/\partial t\}(kT)^{-1}\\&\pm\alpha bn\sum_{i=0}^{\infty}\Delta H_i\exp(-bt^n)t^{n-1}-(1-\alpha)(\eta/t)\\&\times(t/\tau)^{\eta}\sum_{i=0}^{\infty}\Delta H_i\exp[-(t/\tau)^{\eta}]\end{aligned} \tag{11}$$

of $(\partial H/\partial t)_T$ in terms of $t$, which is a directly measured parameter in the present experiments. In this relation, the constant $m+nP$ is normalized to unity. It obviously represents an exothermic (or an endothermic) signal

$$\begin{aligned}(\partial H/\partial t)_T&=\pm\alpha bn\sum_{i=0}^{\infty}\Delta H_i\exp(-bt^n)t^{n-1}\\&=\pm\alpha bn\sum_{i=0}^{\infty}\Delta H_i(1-y)t^{n-1},\end{aligned} \tag{12}$$

with

$$y=1-\exp(-bt^n), \tag{13}$$

showing a peak at a nonzero time

$$t_p=\left[\frac{n-1}{bn}\right]^{1/n} \tag{14}$$

in the predominant contribution $\alpha$ to the H redistribution (or desorption) reaction. Reaction (14) can be derived by solving $\partial y/\partial t=0$ in Eq. (13) in the boundary conditions for an optimum value of the enthalpy $H$ per unit time in the involved reaction. It represents the observed value of $t_p=0.68$ min in the isothermogram at 418 K in Fig. 4(c) with $n=1.6$ and $b=0.702$ min$^{-1.6}$. The value of $n=1.6$ is obtained independently by the partial area analysis of this thermogram. In this method, the different values of $y$, according to Eq. (13), are obtained at different values of $t$ from the observed isothermogram and finally the value of $n$ is obtained by the slope of

the linear plot between $\ln\{-\ln(1-y)\}$ and $\ln t$, as described earlier.[24] A simulation made using these values of $n$ and $b$, with the observed $\Sigma\Delta H_i = 133.5$ J/g, in Eq. (12), yields the best fit to the observed thermogram shown by the dotted curve in Fig. 4(c). A small difference between the two curves occurs at higher $t$ due to the onset of the SR. The SR signal is well described by the third term in Eq. (11), which represents a monotonically decreasing exothermic signal of $(\partial H/\partial t)_T$ with $t$, as evidenced by the simulations in Fig. 9 for three representative isothermograms at (a) 418 K, (b) 583 K, and (c) 523 K. All three thermograms assume the same value of $\eta = 0.6$ with different values of $\tau$ (from 21 to 25 s) and $\Sigma\Delta H_i$ (from 16 to 480 J/g).

For the $(\partial H/\partial t)_T$ versus $T$ isochronal measurements of the H-redistribution reaction (or H desorption) at the heating rate $\beta$, the same relation (11), as used for the isothermal measurements, can be rewritten in terms of $T$ by replacing the $t$ by $T/\beta$ as follows:

$$
\begin{aligned}
(\partial H/\partial t) = & \sum_{i=0}^{\infty} \Delta H_i(T_0)\{\exp[\Delta E_i/kT]\} \\
& \times\{(\partial \Delta E_i/\partial T)\beta(kT)^{-1}\} \pm \alpha bn \sum_{i=0}^{\infty} \Delta H_i \\
& \times \exp\{-b(T/\beta)^n\}(T/\beta)^{n-1} - (1-\alpha)(\beta\eta/T) \\
& \times (T/\beta\tau)^{\eta} \sum_{i=0}^{\infty} \Delta H_i \exp[-(T/\beta\tau)^{\eta}], \qquad (15)
\end{aligned}
$$

which also yields a peak at temperature

$$
T_p = \beta\left[\frac{n-1}{bn}\right]^{1/n} \qquad (16)
$$

for a nondegenerate single process. It can be derived by solving $(\partial^2 H/\partial^2 t) = 0$ as in Eq. (14). It qualitatively describes the evolution of the involved endothermic or exothermic signals in $Nd_2Fe_{14}BH_x$, $x \leqslant 5$, using similar kinetic parameters as in the isothermograms in the isothermal measurements.

## IV. CONCLUSIONS

Thermograms in the desorption of H atoms in $Nd_2Fe_{14}BH_x$, $x \leqslant 5$, microcrystals are studied by heating the specimen in a Perkin-Elmer DSC-7 calorimeter. The H atoms, which occupy the $4c$, $16k2$, $16k1$, $4e$, $8j2$, and $8j1$ crystallographically and energetically inequivalent interstitial sites between Fe atoms in the $P4_2/mnm$ tetragonal crystal unit cell, desorb in successive steps according to their bonding energies in the lattice, showing six endothermic (irreversible) signals over 325–800 K. The intensity (the change in the enthalpy) in the spectrum of the six thermograms varies according to the population of the H atoms in the six sites. As a result, the thermogram in the desorption of H atoms from the $16k2$ (or $16k1$) site, which has the highest occupancy of $n_i(H) = 6$ (or 5) H atoms per $Nd_2Fe_{14}BH_x$, $x \sim 5$, crystal unit cell (with a total of $4x = 20$ H atoms), appears to be the most intense amongst the six thermograms. In an isochronal heating, H atoms in the $16k2$ and $16k1$ sites desorb over the same temperatures, resulting in a single broad thermogram at 439 K (at the heating rate $\beta \sim 15$ K/min). The H desorption from these two sites could be distinguished with the help of a controlled isothermal desorption of the sample by heating it as a function of time at elevated temperature.

Each of the six identified interstitial H sites in $Nd_2Fe_{14}BH_x$, $x \sim 5$, in this investigation involves an independent thermal excitation and activation process of the desorption of H atoms characterized by a separate activation energy, in the range 48–123 kJmol$^{-1}$, as analyzed by the $\beta$ dependence of the peak positions of the thermograms with the modified Kissinger relation.[41] Neutron-diffraction measurements, available for polycrystalline samples of $R_2Fe_{14}B$ deuterides (with $R$ = Y, Ce, or Er) at room temperature, are not sensitive enough to detect the small presence of D or H atoms in the $4c$ and $8j1$ sites.[12] They determine the H occupancies $n_i$(H) in the other four sites in a 26:100:80:54 ratio in a fairly good agreement with those calculated in the 30:100:80:73 ratio by the enthalpies in the four prominent H-desorption thermograms for the $Nd_2Fe_{14}BH_x$, $x \sim 5$, microcrystals. The desorption (or the absorption) of H atoms in the $4c$ and $8j1$ sites induces small changes of $\sim 1$ kOe (15–24 kOe in the other sites) in the magnetic hyperfine fields of the hydride (or the anhydride).[23]

When measured isothermally at elevated temperatures, a monotonically decreasing exothermic signal of the rate of the change of the enthalpy. $(\partial H/\partial t)_T$, as a function of time $t$ follows the primary endothermic H-desorption signal. It is ascribed to the H-desorption-induced structural relaxation, with a relaxation time $\tau \sim 25$ s, of the atoms in the lattice towards the equilibrium configuration after the H atoms are desorbed. The H-desorption process is generally expected to involve classical thermal excitations of H atoms in the localized H energy levels (in the local bonding with the lattice) in the interstitial sites, which influence the equilibrium positions of the atoms in the lattice at the moment they jump off the lattice by causing an instantaneous change in the momentum of the system. The final atoms in the lattice subsequently relax towards their equilibrium positions in the lattice by releasing the excess configurational energy (an exothermic signal) with $t$, after H desorption at $t = 0$. The simulations obtained with an existing formalism of the structural relaxations[42,43] successfully represent the results.

A significant portion of H atoms, thermally excited to high-energy levels in the interstitial sites in the process to the desorption, redistribute over the neighboring sites by modifying the interstitial energies and $n_i(H)$ values at high temperatures. The isochronal desorption of H atoms from the $4c$ site in $Nd_2Fe_{14}BH_x$, $x \sim 5$, presents a good example of it. Thus, at a slow heating ($\beta \leqslant 40$ K/min) from room temperature, the H atoms in this site slowly tunnel to neighboring higher-transition-energy ($kT$) sites at the expense of the desorption in the low-temperature H-desorption thermal signal at $\sim 340$ K. As a result, the intensity (the change in the enthalpy) in this signal is found to be progressively increasing with increasing $\beta$ in the range 10–100 K/min. A sample scanned at $\beta \sim 15$ K/min allows a sufficient time to perform the redistribution reactions over the various sites, showing a decreased value of $\Delta H$ from 368 J/g at $\beta = 100$ K/min to 249 J/g at $\beta \sim 15$ K/min in a decreased total H desorption over 300–800 K. The H-redistribution reaction is exothermic. It

could be studied separately in a partially H desorbed sample (at 583 K for 90 min and cooled to 303 K), which exhibits two weak exothermic signals at 616 and 684 K (at $\beta = 50$ K/min), with a total $\Delta H$ of 9.5 J/g only, in the H redistributions in the high-energy interstitial sites $8j2$ and $8j1$, respectively. The last H atoms in the sample desorb as a two-step endothermic H-desorption signal in an isothermal heating at a further higher temperature of 720 K.

## ACKNOWLEDGMENT

This work was financially supported (S.R.) by the Alexander von Humboldt Foundation, Germany.

*Permanent address: Materials Science Centre, Indian Institute of Technology, Kharagpur 721302, India.

[1] S. Hirosawa, Y. Matsuura, H. Yamamoto, S. Fujimura, M. Sagawa, and H. Yamauchi, J. Appl. Phys. **59**, 873 (1986).
[2] M. Yamada, H. Kato, H. Yamamoto, and Y. Nakagawa, Phys. Rev. B **38**, 620 (1988).
[3] M. C. D. Deruelle, M. Yamada, H. Yamauchi, and Y. Nakagawa, Phys. Rev. B **42**, 10 291 (1990).
[4] D. W. Lim, H. Kato, M. Yamada, G. Kido, and Y. Nakagawa, Phys. Rev. B **44**, 10 014 (1991).
[5] J. F. Herbst, Rev. Mod. Phys. **63**, 819 (1991).
[6] M. R. Ibarra, L. Pareti, P. A. Algarabel, L. Morellon, C. Marquina, and M. Solzi, J. Phys., Condens. Matter. **5**, 5637 (1993).
[7] D. Givord, H. S. Li, and B. R. Perrier, Solid State Commun. **51**, 857 (1984).
[8] F. Bolzoni, J. P. Gavigan, D. Givord, H. S. Li, O. Moze, and L. Pareti, J. Magn. Magn. Mater. **66**, 158 (1987).
[9] J. Bartolome, F. Luis, D. Fruchart, O. Isnard, S. Miraglia, S. Obbade, and K. J. H. Buschow, J. Magn. Magn. Mater. **101**, 411 (1991).
[10] D. Fruchart, S. Miraglia, S. Obbade, P. Ezekwenna, and P. l'Heritier, J. Magn. Magn. Mater. **83**, 291 (1990).
[11] S. Ram and J. C. Joubert, Appl. Phys. Lett. **61**, 613 (1992); J. Appl. Phys. **72**, 1164 (1992).
[12] P. Dalmas de Reotier, D. Fruchart, L. Pontonnier, F. Vaillant, P. Wolfers, A. Yaouanc, J. M. D. Coey, R. Fruchart, and P. l'Heritier, J. Less-Common Met. **129**, 133 (1987).
[13] J. M. D. Coey, A. Yaouanc, D. Fruchart, R. Fruchart, and P. l'Heritier, J. Less-Common Met. **131**, 419 (1987).
[14] J. R. Regnard, A. Yaouanc, D. Fruchart, D. Le Roux, P. l'Heritier, J. M. D. Coey, and J. P. Gavigan, J. Appl. Phys. **61**, 3565 (1987).
[15] L. Y. Zhang, F. Pourarian, and W. E. Wallace, J. Magn. Magn. Mater. **71**, 203 (1988).
[16] D. Fruchart, L. Pontonnier, F. Vaillant, J. Bartolome, J. M. Fernandez, J. A. Puertolas, C. Rillo, J. R. Regnard, A. Yaouanc, R. Fruchart, and P. l'Heritier, IEEE. Trans. Magn. **MAG-24**, 1641 (1988).
[17] B. Rupp, A. Resnik, D. Shaltiel, and P. Rogl, J. Mater. Sci. **23**, 2133 (1988).
[18] L. Pareti, O. Moze, D. Fruchart, P. l'Heritier, and A. Yaouanc, J. Less-Common Met. **142**, 187 (1988).
[19] E. Claude, S. Ram, I. Gimenez, P. Chaudouet, D. Boursier, and J. C. Joubert, IEEE Trans. Magn. **MAG-29**, 2767 (1993).
[20] S. Ram, E. Claude, and J. C. Joubert, IEEE Trans. Magn. **MAG-31**, 2200 (1995).
[21] S. Ram, M. Febri, H. J. Fecht, and J. C. Joubert, Nanostruct. Mater. **6**, 473 (1995).
[22] S. Ram, J. Mater. Sci. (to be published).
[23] J. M. Cadogan and J. M. D. Coey, Appl. Phys. Lett. **48**, 442 (1986).
[24] S. Ram, Phys. Rev. B **49**, 9632 (1994).
[25] H. J. Fecht, Z. Fu, and W. L. Johnson, Phys. Rev. Lett. **64**, 1753 (1990).
[26] J. N. Daou, J. P. Burger, and P. Vajda, Philos. Mag. B **65**, 127 (1992).
[27] C. E. Krill, J. Li, W. B. Yelon, and W. L. Johnson, Phys. Rev. B **48**, 3689 (1993).
[28] P. Vajda and J. N. Daou, Phys. Rev. B **49**, 3275 (1994).
[29] C. Schönfeld, R. Hempelmann, D. Richter, T. Springer, A. J. Dianoux, J. J. Rush, T. J. Udovic, and S. M. Bennington, Phys. Rev. B **50**, 853 (1994).
[30] K. J. H. Buschow, Mater. Sci. Rep. **1**, 1 (1986).
[31] L. Schultz, K. Schnitzke, J. Wecker, M. Katter, and C. Kuhrt, J. Appl. Phys. **70**, 6339 (1991).
[32] C. D. Fuerst and E. G. Brewer, J. Appl. Phys. **73**, 5751 (1993).
[33] C. D. Fuerst, E. G. Brewer, R. K. Mishra, Y. Zhu, and D. O. Welch, J. Appl. Phys. **75**, 4208 (1994).
[34] X. C. Kou, H. Kronmüller, D. Givord, and M. F. Rossignol, Phys. Rev. B **50**, 3849 (1994).
[35] I. Ahmad, M. A. Al-Khafaji, H. A. Davies, W. M. Rainforth, and R. A. Buckley, J. Magn. Magn. Mater. **145**, L-19 (1995).
[36] Y. Zhu, J. Tafto, L. H. Lewis, and D. O. Welch, Philos. Mag. B **71**, 297 (1995).
[37] J. F. Herbst, J. J. Croat, F. E. Pinkerton, and Y. B. Yellon, Phys. Rev. B **29**, 4176 (1984).
[38] C. B. Shoemaker, D. P. Shoemaker, and R. Fruchart, Acta Crystallogr. Sec. C **40**, 1665 (1984).
[39] T. S. Chin, H. J. Bai, K. D. Lin, F. D. King, and S. J. Heh, J. Appl. Phys. **70**, 6600 (1991).
[40] H. E. Kissinger, Anal. Chem. **29**, 1702 (1957).
[41] J. A. Augis and J. D. Bennett, J. Therm. Anal. **13**, 283 (1978).
[42] S. Ram, Phys. Rev. B **42**, 9582 (1990).
[43] S. Ram and G. P. Johari, Philos. Mag. B **61**, 299 (1990).
[44] M. Kemali, R. L. Havil, and M. Titman, Philos. Mag. B **72**, 275 (1995).